Self-Propelled Polymer Multilayer Janus Capsules for Effective Drug Delivery and Light-Triggered Release

Yingjie Wu,[†] Xiankun Lin,*[,†] Zhiguang Wu,[†] Helmuth Möhwald,[‡] and Qiang He*[,†]

[†]State Key Lab of Urban Water Resource and Environment (HIT), Micro/Nanotechnology Research Centre, Harbin Institute of Technology, Harbin 150080, China

[‡]Max-Planck Institute of Colloids and Interfaces, Potsdam D-14424, Germany

S *Supporting Information*

ABSTRACT: We present herein a novel hybrid, polymer-based motor that was fabricated by the template-assisted polyelectrolyte layer-by-layer (LbL) deposition of a thin gold layer on one side, followed by chemical immobilization of a catalytic enzyme. Such Janus capsule motors can self-propel at 0.1% peroxide fuel concentration at physiological temperature and have a higher speed as compared to Pt-based synthetic motors. They were exploited for encapsulation of the chemotherapeutic anticancer drug, doxorubicin, for navigation to target a cell layer by an external magnetic field, and for triggered drug release activated by NIR light. This work provides high potential in the development of multifunctional polymer-based engines for biomedical applications such as targeted drug delivery.

KEYWORDS: layer-by-layer, autonomous motor, Janus capsules, biocatalysis, remote release
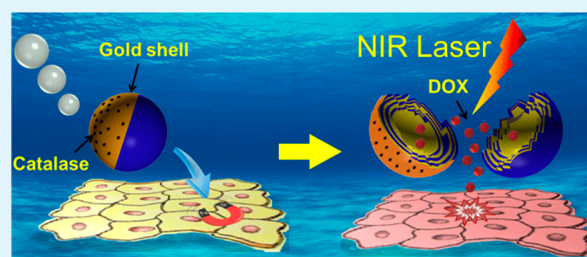
INTRODUCTION

The development of new-generation drug delivery vehicles capable of encapsulating, transporting, and releasing substances in a rapid and controlled manner is of great interest.[1−4] Particularly, these new delivery vehicles are able to integrate self-driven and navigation capabilities so that they may achieve not only smart encapsulation and release but also precise guidance and control. Inspired by the movement of biomolecular motors such as kinesins, particular attention has been paid to chemically powered, self-propelled catalytic micro-/nanomotors (e.g., metal nanorods, Janus silica particles, and metal/conductive polymer microtubes), which can convert chemical energy into movement and forces.[5−11] They have been shown to enable the pick-up, transportation, and release of various cargoes including polymer particles, cancer cells, nucleic acid, and bacteria.[12−15] However, the use of these synthetic motors for directed drug transportat suffers from poor biocompatibility and biodegradability, complex preparation technology, difficulty of manipulation and multifunctionaliza-tion, weak motion control, poor cargo loading, transport, and release.[16−19] Recently, chemically powered, polymer-based motors have greatly enhanced the prospects for drug delivery application of nanomachines. For example, van Hest and co-workers developed autonomous bowl-shaped polymer stoma-tocytes, which utilize the controlled deformation of polymer vesicles to selectively entrap platinum nanoparticles within their nanocavities and subsequently use catalysis as a driving force for movement.[20] Similarly, He and co-workers described self-driven platinum nanoparticle-modified polymer multilayer capsules and tubes, which can serve as both efficient catalytic motors and

smart cargos.[21] Such an impressive progress promises sophisticated drug delivery. However, these studies did not address the issues of high power conversion, loading, targeting, and release.

Self-propelled synthetic motors hold great potential in diverse fields, such as biomedical fields. Basically, a successful motor system that can be applied in biomedical fields has to resolve at least four changing points as follows: (1) The first is biocompatibility and biodegradability of motor materials. In this Article, we used polymers, gold, and enzyme as the assembling materials to prepare capsule motors because all of them are biocompatible or biodegradable. (2) Next is easy multifunctionality. The use of LbL technique to prepare capsule motors can easily incorporate various assembling units into the capsule walls and further realize the multifunctionality on demand. Thus, the exposed capsule side can be tailored to be responsive to different chemical, physical, and biological stimuli. On the other hand, gold can be used for immobilization of enzymes, generation of Janus structure, and finally serve as a NIR-responsive agent to perform photothermal treatment. (3) Third is velocity and direction. The velocity could be tuned by the fuel concentration and temperature as proved in this Article and other previous reported. Also, the direction can be navigated by a remotely magnetic operation. 4) The final is fuels or driving forces. Basically, the employed fuels or driving forces should be friendly to biological systems. Here, we have

successfully performed the in vitro cell experiments at a very low peroxide concentration (i.e., 0.2%), and almost 100% of HeLa cells remain alive for more than 3 h. Although the peroxide fuel employed for self-propulsion is still toxic to sustain mammalian cellular functions, biocompatible fuels or alternative powered methods can be employed in the future.

This is the aim of this study, where we demonstrate the rapid transportation of capsule motors toward targeted cancer cells. This is driven by the biocatalytic decomposition at low concentration of peroxide fuel (0.1–2%, v/v) at physiological temperature and subsequent light-triggered anticancer drug release in a controlled manner (Figure 1A). In this
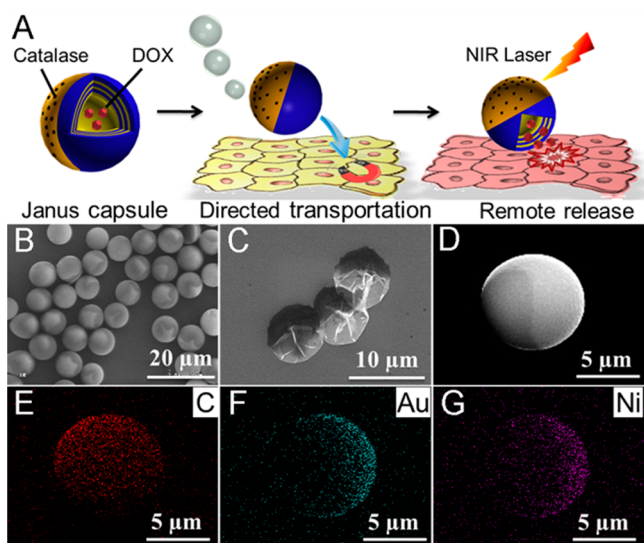

Figure 1. (A) Scheme of the targeted movement and light-triggered drug release of Janus capsule motors. (B,C) SEM images of Janus motors before and after removal of the SiO_2 cores. (D−G) SEM image and corresponding EDX mapping analysis of a Janus motor before removal of the template.

concentration range, where the fuel is still biocompatible, the enzyme-functionalized Janus capsule motors move at a higher speed as compared to the known Pt-based motors.[22] The Janus capsule motors fabricated by the versatile layer-by-layer (LbL) multilayer assembly possess outstanding delivery capacities, preserve the function of various building units, and sensitively respond to various stimuli for controllable encapsulation and release of drugs or other components.[23−27] We envision that this self-propelled Janus polymer multilayer capsule motor displays potential for developing multifunctional polymer-based engines, performing highly efficient drug encapsulation, and remotely controlled release and targeted transportation.

■ EXPERIMENTAL SECTION

Materials. The silica spheres with diameter of 8 μm were obtained from Microparticles GmbH, Berlin, Germany. Poly(styrenesulfonate) sodium salt (PSS, M_w = 70 000), poly(allylamine hydrochloride) (PAH, M_w = 70 000), fluorescein isothiocyanate (FITC), FITC-dextran, benzalkonium chloride, 3-mercaptopropionic acid, 1-ethyl-3-[3-(dimethylamino)propyl] carbodiimide hydrochloride (EDC), *N*-hydroxylsulfosuccinimide (Sulfo-NHS), doxorubicin (DOX), and PBS (pH 7.2) were purchased from Sigma-Aldrich. Sodium chloride (NaCl), hydrofluoric acid (HF), and hydrogen peroxide (H_2O_2) were used without further purification. FITC-modified PAH (FITC-PAH) was prepared through labeling PAH with FITC according to the literature. The water used in all experiments was prepared by using a

Milli-Q purification system enabling a resistivity higher than 18.2 MΩ cm^{-1}.

Preparation of Catalase-Coated LbL-Assembled Capsules. $(PSS/PAH)_5$-coated particles were first prepared by the layer-by-layer assembly of polyelectrolyte layers on the surface of SiO_2 particles with a diameter of 8 μm. The SiO_2 particles were alternately suspended in PSS and PAH solutions, both of which have a concentration of 2 mg/mL and contain 0.5 M NaCl, for 15 min under continuous shaking, followed by three repeated centrifugation/washing steps. The (PSS/PAH)$_5$-coated silica particles were obtained by repeating the above deposition procedure, and the outer layer was PAH. To fabricate the Janus structures, we first drop casted a 3 mL colloidal suspension of polyelectrolyte modified silica particles (diluted in ethanol with a 1:5 ratio) onto a clean silicon wafer tilted at an angle of about 9°. The monolayer was dried via slow evaporation of the solvent at room temperature, which allows the beads to spread into a self-assembled monolayer. The particle-coated substrates were loaded into a vacuum chamber, and a 2 nm Cr adhesion layer, 5 nm Ni, and 5 nm Au layer were deposited at a vapor incidence angle of 30°, resulting in roughly half-coated beads. The microparticles then were separated into aqueous solution.

The outer Au layer of the coated microparticles was functionalized first with a 2.5 mM ethanol solution of 3-MPA overnight at room temperature. After the particles wree rinsed with water for 5 min, the modified microparticles were subsequently treated with a solution of Sulfo-NHS (100 mM) and EDC (400 mM) in PBS (pH 7.2) for 12 h. Further incubation for 12 h at 37 °C in a catalase (2 mg/mL) solution (prepared in 0.1 M PBS of pH 7.2) was followed by three rinsing steps with PBS solution. Finally, the silica cores were dissolved by treatment with 1 M HF (Caution: HF is extremely toxic and can penetrate the skin!). The capsules were purified by three centrifugation/water washing steps. All obtained capsule solutions were stored at 4 °C until use.

Permeability Investigation of the Capsules. Confocal laser scanning microscopy (CLSM) was used to check the permeability of capsules. FITC-labeled dextran with different molecular weights (M_w = 4000 and 10 000 Da) was used for testing. For comparison, the capsule suspensions with the same volume and concentration were mixed with two kinds of FITC-dextran (2 mg/mL), respectively.

Magnetic Navigation of Janus Motors. To magnetically operate the Janus $(PAH/PSS)_5$ capsule motor, an external weak magnetic field of about 0.02 T was applied by placing a small magnet at 5 cm away from the glass slide without changing the distances. Changing the direction of the magnet, the Ni cap will follow the orientation of the magnetic field. The direction of the Janus motor was also navigated under an external magnetic field of 0.02 T to approach the targeted HeLa cells. The manipulations of the Janus motors and their motion were tracked using a microscope.

NIR Laser-Triggered Release of DOX from the Janus Capsule Motors in Vitro. A standard cell culture procedure was used. Briefly, the HeLa cells were incubated in Dulbecco's Modified Eagle Medium (DMEM) supplemented with 10% fetal bovine serum (FBS) and 1% penicillin-streptomycin at 37 °C in an atmosphere of 5% CO_2. The cells in the logarithmic growth phase were seeded into 60 mm polystyrene (PS) plates at a cell density of about 2×10^4 cells per plate for test. Subsequently, the medium was removed, and the cells were coincubated with Janus motors (400 μg) in the solution of 0.5% H_2O_2 (500 μL). Under navigation by the external magnetic field, the autonomous motors were directed to the predetermined destination. When most motors were bound to the cells, a near-infrared laser (808 nm) at power of 13 mW μm^{-2} for 30 s was used to trigger the unloading process. The process was investigated by optical microscopy and the fluorescence microscopy of the HeLa cells and Janus motors before and after the treatment.

Characterization. For scanning electron microscopy (SEM) (Hitachi S-5200) observation, a drop of the sample solution was dropped onto a silicon wafer and dried at room temperature for the test. Transmission electron microscopy (TEM) and energy-dispersive X-ray spectroscopic (EDX) analyses were performed using a Tecnai G2 F30 microscope. Copper grids sputtered with carbon films were

used to support the sample. Fluorescence images were obtained using a Leica TCS SP5 II confocal laser scanning microscope (CLSM). The excitation wavelength was 488 nm for the excitation of FITC. An Olympus BX53 fluorescence microscope coupled with a 40× objective and relative software was employed to record the motion of capsule motors and the interaction between Janus motor and HeLa cancer cells. The trajectories of the Janus capsule motors were analyzed by ImageJ software.

■ RESULTS AND DISCUSSION

The versatile LbL assembly allows on-demand fabrication of polymer-based capsules by deposition of different materials. First, five bilayers of negatively charged poly(styrenesulfonate) (PSS) and positively charged poly(allylamine hydrochloride) (PAH) were alternatingly absorbed on the surface of 8 μm silica particles according to procedures previously reported.[28−30] Second, a drop of $(PSS/PAH)_5$-coated silica particles was spread on a flat silicon substrate to form a monolayer, and then 5 nm thickness nickel and 5 nm gold were subsequently sputtered onto the particle monolayer. After removal of the silica template, hollow Janus $(PSS/PAH)_5$ capsules were obtained. Finally, the outer Au layer was functionalized with self-assembled monolayers (SAMs) of 3-mercaptopropionic acid (3-MPA). The carboxylic terminal groups of the SAMs were converted to amine-reactive esters for covalent binding of catalase by using the coupling agents 1-ethyl-3-[3-(dimethylamino)propyl] carbodiimide hydrochloride (EDC) and N-hydroxylsulfosuccinimide (sulfo-NHS). As each catalase molecule can decompose millions of hydrogen peroxide molecules per second, it was chosen as biocatalyst.

The preparation and structure of the Janus motors were characterized systematically. The scanning electron microscopic (SEM) image of Figure 1B shows LbL-coated silica particles after sputtering with Ni and Au. One can see that the metal cap with irregular edge partially covers the polymer-coated particles, providing them a Janus feature. Furthermore, the scanning electron microscopic (SEM) images and corresponding energy-dispersive X-ray spectroscopic (EDX) mapping (Figure 1D−G) confirm the existence and asymmetric distribution of metal. In addition, the thickness of the metal layer is heterogeneous; that is, the metal caps have more metal on the top than on the edge. After removal of the silica cores, the Janus capsules with the partly coated metal layer can be obtained as shown in Figure 1C. FITC-PAH was used to label the polyelectrolyte capsules. Both fluorescence and confocal laser scanning microscopic (CLSM) images (Supporting Information Figure 1A,B) indicate that the metal layer has been immobilized on the capsule motors.

The LbL-assembled polyelectrolyte multilayer capsules usually possess high loading ability and selectivity, which makes them excellent vehicles for drug delivery.[31−33] The encapsulation of the targeted substances can be easily realized by selectively tuning the permeability of the capsule walls through chemical, biological, and physical stimuli.[34] To explore the permeability of the as-prepared Janus capsules, fluorescein isothiocyanate-dextran (FITC-dextran) with different molecular weight was chosen as model compound. When capsules are exposed to FITC-dextran (4 kDa) solutions, the fluorescence intensity of their interior and exterior becomes almost identical in a short time, indicating that FITC-dextran (4 kDa) molecules can easily pass through the wall of these hollow Au-coated $(PAH/PSS)_5$ capsules (Figure 2A). On the contrary, when FITC-dextran with molecular weight of 10 kDa is
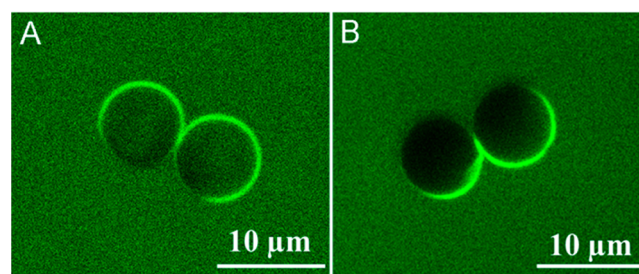

Figure 2. CLSM images of Janus capsule motors after incubation with FITC-dextran with a molecular weight of 4 kDa (A) and 10 kDa (B), respectively.

employed, the capsule interior remains dark over longer time and obviously is impermeable to FITC-dextran (10 kDa) (Figure 2B). These results show that after metal coating and surface modification, the Janus $(PAH/PSS)_5$ capsules maintain the selective permeability like the well-studied $(PAH/PSS)_5$ capsules.[35] We can thus adapt the reported encapsulation methods for the $(PAH/PSS)_5$ capsules to load the drug molecules inside the Janus $(PAH/PSS)_5$ capsules.

Figure 3A−C displays time-lapse images, taken from Supporting Information video 1, for the movement of a Janus
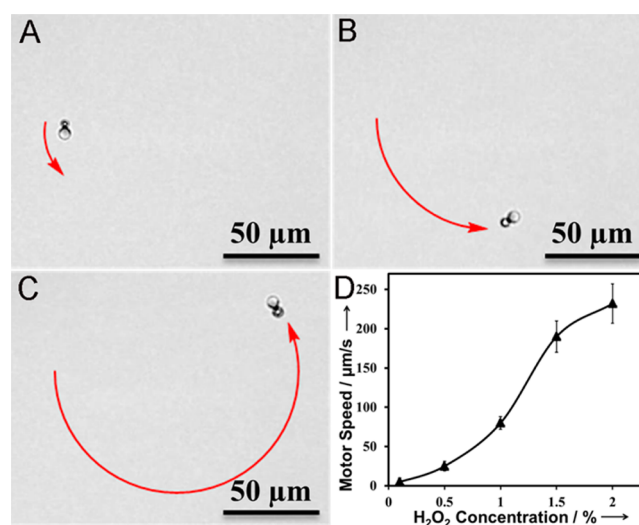

Figure 3. (A−C) Time-lapse images for self-propulsion of the Janus $(PSS/PAH)_5$ capsule motor in 1% H_2O_2 solution at 37 °C, recorded by an optical microscope. The red arrows indicate the trajectory of the Janus motor. (D) Fuel concentration dependence of the average speed of the Janus capsule motors for the range of 0.1−2% H_2O_2 at 37 °C.

$(PAH/PSS)_5$ capsule motor in a 1% H_2O_2 solution containing 0.001 wt % benzalkonium chloride at 37 °C. The bigger dot with asymmetric shape represents a Janus capsule motor, and the smaller one corresponds to an oxygen bubble. One can see that the generation, growth, and detachment of the oxygen bubbles occur on the Pt-capped side of the capsule motor (i.e., dark region). The movement of the Janus capsule motor is directed opposite to the bubble detachment, showing that the capsule motion is propelled by the oxygen bubbles. Also, the motor shows a circular motion with a speed of 108 μm/s (14 body lengths/s) in this case. Such pronounced speeds are ascribed to the asymmetric distribution of the catalase on the surface of Janus $(PAH/PSS)_5$ capsules and its high catalytic efficiency as compared to platinum (Pt).[7] The average speed of

10478

dx.doi.org/10.1021/am502458h | ACS Appl. Mater. Interfaces 2014, 6, 10476−10481

the capsule motors decreases from ~232 μm/s at 2% H_2O_2 (29 body lengths/s, 90% of Janus microcapsule motors remain active) to 4.2 μm/s at 0.1% H_2O_2 (half a body length/s, 40% of Janus microcapsule motors remain active) (Figure 3D). The monotonous dependence on fuel concentration demonstrates that the velocity of the Janus capsule motors can be readily modulated through changing the concentration of the fuel. More interestingly, the capsule motor still exhibits a force of 0.4 pN at 0.1% H_2O_2 according to the Stokes law ($F_{drag} = 6\pi\mu rv$),[21] indicating that a sufficient amount of drugs could still be loaded and transported by these synthetic microengines. It is noted that at such low peroxide concentrations, the speed of our capsule motors obtained at 37 °C is substantially higher than that of previously reports for room temperature.[21] In addition, the effective self-propelled motion of the Janus (PAH/PSS)$_5$ capsule motors at low H_2O_2 concentration is helpful to reduce the toxicity of peroxide fuel for living cells or organisms.

Both controllable transportation of the drug carriers and subsequently triggered release of the loaded drugs in a remote way are essential in the field of targeted drug delivery. To direct the motion in solution, we sputtered a magnetic nickel (Ni) film with a thickness of 5 nm on the Janus capsule motors before Au deposition. We expect that this could provide well-defined anisotropic magnetic properties of the Janus capsule motors and enables us to navigate the orientation of Janus particles at the microscale using a magnet, but not change their location. Figure 4 and Supporting Information video 2 show
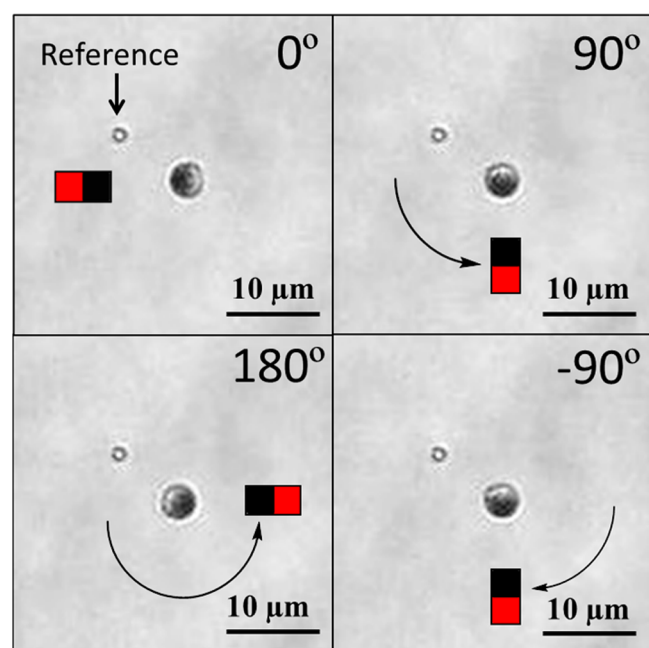

Figure 4. Time-lapse image of manipulating the orientation of a Janus (PAH/PSS)$_5$ capsule motor by changing the direction of a magnet with a magnetic field of about 0.02 T; the central region of the motor does not change its location.

that the Ni-coated cap of a Janus capsule motor follows the orientation as compared to a reference dust particle upon applying an external magnetic field of about 0.02 T. We did not observe any displacement of the Janus capsule during the manipulation experiment, implying that the intensity of the external magnetic field is relatively weak and can be neglected. A 0.02 T magnetic field then was applied for the following

navigation experiment. Figure 5 shows time-lapse images captured from a video (Supporting Information video 3) for
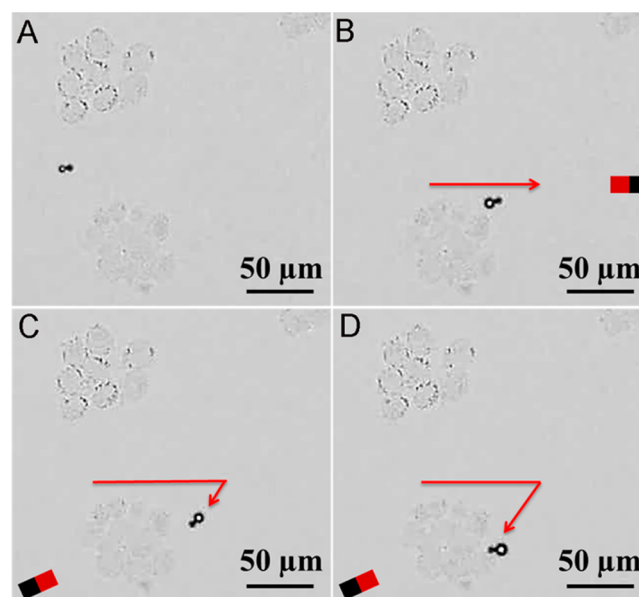

Figure 5. (A−D) Time-lapse images of the targeted transport of a single Janus (PSS/PAH)$_5$ capsule motor to HeLa cells under external magnetic guidance in 0.5% H_2O_2 at 37 °C. The red lines show the trajectories.

the motion of a single Janus (PSS/PAH)$_5$ capsule motor toward HeLa cells in 0.5% H_2O_2 solution. HeLa cells were found to survive for more than 60 min in 0.5% H_2O_2 solution and did not obviously change their shape. Initially, the as-assembled Janus (PSS/PAH)$_5$ capsule motor swam randomly at a speed of 25 μm/s (about 3 body lengths per second). Under an external magnetic field, the movement of the Janus capsule motor was navigated to approach the targeted HeLa cells. Once the Janus capsule had attached to the HeLa cell, it did not detach from the cell due to the electrostatic attraction between the negatively charged HeLa cell membrane and the positively charged outer layer (PAH) of the Janus capsule motor.

Previous studies have demonstrated that near-infrared (NIR) light could trigger the shell breakage of gold nanoparticle-modified polymer multilayer capsules and rapidly release the encapsulated substances.[36] Similarly, we also applied NIR light as an external physical stimulus to trigger the release of the encapsulated drug in the Janus capsule after it attached onto the HeLa cells. To better observe the drug release, a fluorescent anticancer drug, doxorubicin (DOX), was chosen as a model drug and encapsulated into the Janus capsules through encapsulation from an organic solvent.[37] This method is based on the fact that an organic solvent will partially break the electrostatic attraction between PAH and PSS, and then the permeability of the polyelectrolyte multilayer capsules is largely increased. Therefore, when alcohol was injected into the mixed aqueous solution of Janus capsules and DOX for 30 min and then alcohol was removed by centrifugation, a certain amount of DOX was loaded inside the Janus capsules. Furthermore, UV−visible spectroscopy reveals that about 1.25 ng of DOX has been encapsulated in a capsule motor.

The images of differential interference contrast (DIC), CLSM, scanning electron microscope (SEM), in Figure 6 show the corresponding results before and after NIR laser
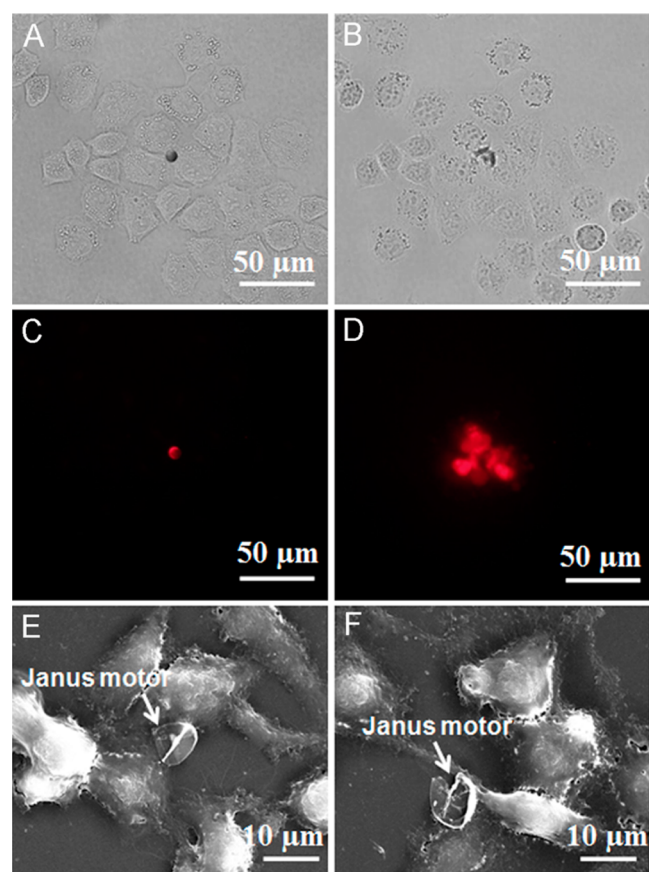
Figure 6. Remote controlled release of DOX from the Janus capsule motors into HeLa cells by using NIR light at 808 nm at a power output of 13 mW μm^{-2}. DIC, fluorescence microscope, and SEM images of (A,C,E) before and (B,D,F) after NIR irradiation.

illumination. Figure 6A,C,E demonstrates that if a Janus (PSS/PAH)$_5$ capsule binds to the HeLa cell sheet, it still remains intact. The red color in Figure 6C is due to fluorescence of DOX, indicating its successful encapsulation inside the Janus capsule. After irradiation with NIR light, the Janus (PSS/PAH)$_5$ capsule was partially ruptured (Figure 6B,F). The thus released DOX molecules then penetrated into the surrounding HeLa cells, which causes the color change of these HeLa cells (Figure 6D). The NIR laser-induced release is attributed to the produced heat pulse on the side of the gold-coated Janus (PSS/PAH)$_5$ capsules. Upon NIR laser irradiation of the plasmon resonance of a structured gold layer, electromagnetic energy is absorbed and dissipated as heat into the surrounding media. Also, gold shells show excellent potential for offering "on-demand" release in response to NIR excitation by changing the surface roughness and the thickness of the Au shell. The heat-induced release has been already demonstrated[36] for this polymeric multilayer, and our measurements show that such a light-activation method can also be integrated into the Janus capsule motors. Therefore, triggered release of the encapsulated drug can be achieved in a remotely controlled manner.

CONCLUSIONS

We have introduced a novel hybrid biocatalytic Janus motor based on hollow polyelectrolyte multilayer capsules and a catalytic enzyme. These enzyme-functionalized Janus capsule motors can be propelled by the biocatalytic decomposition of peroxide fuel, and subsequently the encapsulated drug can be

rapidly released at predefined sites by NIR light triggering. As compared to Pt catalysts, the use of enzymes leads to more powerful and efficient polymer-based motors, allowing use lower peroxide concentrations at physiological temperature. Our Janus polymer-based capsule motors integrate self-driven and navigation capabilities and thus can perform drug loading, targeted transportation, and remotely controlled release in the vicinity of cells and tissues in an organism. Therefore, such self-propelled polymer multilayer capsule motors hold great promise for development of new-generation drug delivery vehicles.

ASSOCIATED CONTENT

Ⓢ Supporting Information

Additional figure and videos. This material is available free of charge via the Internet at http://pubs.acs.org.

AUTHOR INFORMATION

Corresponding Authors
*E-mail: xiankunlin@hit.edu.cn.
*E-mail: qianghe@hit.edu.cn.

Notes
The authors declare no competing financial interest.

REFERENCES

(1) Langer, R.; Tirrell, D. A. Designing Materials for Biology and Medicine. *Nature* **2004**, *428*, 487−492.

(2) Kloxin, A. M.; Kasko, A. M.; Salinas, C. N.; Anseth, K. S. Photodegradable Hydrogels for Dynamic Tuning of Physical and Chemical Properties. *Science* **2009**, *324*, 59−63.

(3) Choi, H. S.; Liu, W. H.; Liu, F. B.; Nasr, K.; Misra, P.; Bawendi, M. G.; Frangioni, J. V. Design Considerations for Tumour-Targeted Nanoparticles. *Nat. Nanotechnol.* **2010**, *5*, 42−47.

(4) Chauhan, V. P.; Jain, R. K. Strategies for Advancing Cancer Nanomedicine. *Nat. Mater.* **2013**, *12*, 958−962.

(5) Paxton, W. F.; Kistler, K. C.; Olmeda, C. C.; Sen, A.; St. Angelo, S. K.; Cao, Y. Y.; Mallouk, T. E.; Lammert, P. E.; Crespi, V. H. Catalytic Nanomotors: Autonomous Movement of Striped Nanorods. *J. Am. Chem. Soc.* **2004**, *126*, 13424−13431.

(6) Fournier-Bidoz, S.; Arsenault, A. C.; Manners, I.; Ozin, G. A. Synthetic Self-Propelled Nanorotors. *Chem. Commun.* **2005**, *4*, 441−443.

(7) Gibbs, J. G.; Zhao, Y. P. Autonomously Motile Catalytic Nanomotors by Bubble Propulsion. *Appl. Phys. Lett.* **2009**, *94*, 163104.

(8) Mei, Y. F.; Huang, G. S.; Solovev, A. A.; Urena, E. B.; Monch, I.; Ding, F.; Reindl, T.; Fu, R. K. Y.; Chu, P. K.; Schmidt; Versatile, O. G. Approach for Integrative and Functionalized Tubes by Strain Engineering of Nanomembranes on Polymers. *Adv. Mater.* **2008**, *20*, 4085−4090.

(9) Wu, Z. G.; Wu, Y. J.; He, W. P.; Lin, X. K.; Sun, J. M.; He, Q. Self-Propelled Polymer-Based Multilayer Nanorockets for Transportation and Drug Release. *Angew. Chem., Int. Ed.* **2013**, *52*, 7000−7003.

(10) Wang, J.; Gao, W. Nano/Microscale Motors: Biomedical Opportunities and Challenges. *ACS Nano* **2012**, *6*, 5745−5751.

(11) Mei, Y. F.; Solovev, A. A.; Sanchez, S.; Schmidt, O. G. Rolled-up Nanotech on Polymers: from Basic Perception to Self-Propelled Catalytic Microengines. *Chem. Soc. Rev.* **2011**, *40*, 2109−2119.

(12) Sundararajan, S.; Lammert, P. E.; Zudans, A. W.; Crespi, V. H.; Sen, A. Catalytic Motors for Transport of Colloidal Cargo. *Nano Lett.* **2008**, *8*, 1271−1276.

(13) Balasubramanian, S.; Kagan, D.; Hu, C. M.; Campuzano, S.; Lobo-Castañon, M. J.; Lim, N.; Kang, D. Y.; Zimmerman, M.; Zhang, L.; Wang, J. Micromachine-Enabled Capture and Isolation of Cancer Cells in Complex Media. *Angew. Chem., Int. Ed.* **2011**, *50*, 4161−4164.

(14) Kagan, D.; Campuzano, S.; Balasubramanian, S.; Kuralay, F.; Flechsig, G.; Wang, J. Functionalized Micromachines for Selective and Rapid Isolation of Nucleic Acid Targets from Complex Samples. *Nano Lett.* **2011**, *11*, 2083−2087.

(15) Zhao, G. J.; Sanchez, S.; Schmidtbc, O. G.; Pumera, M. Micromotors with Built-in Compasses. *Chem. Commun.* **2012**, *48*, 10090−10092.

(16) Gao, W.; Sattayasamitsathit, S.; Manesh, K. M.; Weihs, D.; Wang, J. Magnetically Powered Flexible Metal Nanowire Motors. *J. Am. Chem. Soc.* **2010**, *132*, 14403−14405.

(17) Sengupta, S.; Ibele, M. E.; Sen, A. Fantastic Voyage: Designing Self-Powered Nanorobots. *Angew. Chem., Int. Ed.* **2012**, *51*, 8434−8445.

(18) Ebbens, S. J.; Howse, J. R. In Pursuit of Propulsion at the Nanoscale. *Soft Matter* **2010**, *6*, 726−738.

(19) Song, W. X.; Möhwald, H.; Li, J. B. Movement of Polymer Microcarriers Using a Biomolecular Motor. *Biomaterials* **2010**, *31*, 1287−1292.

(20) Wilson, D. A.; Nolte, R. J. M.; van Hest, J. C. M. Autonomous Movement of Platinum-Loaded Stomatocytes. *Nat. Chem.* **2012**, *4*, 268−274.

(21) Wu, Y. J.; Wu, Z. G.; Lin, X. K.; He, Q.; Li, J. B. Autonomous Movement of Controllable Assembled Janus Capsule Motors. *ACS Nano* **2012**, *6*, 10910−10916.

(22) Orozco, J.; García-Gradilla, V.; Agostino, M. D.; Gao, W.; Cortés, A.; Wang, J. Artificial Enzyme-Powered Microfish for Water-Quality Testing. *ACS Nano* **2012**, *7*, 818−824.

(23) Ariga, K.; Yamauchi, Y.; Rydzek, G.; Ji, Q. M.; Yonamine, Y.; Wu, K. C. W.; Hill, J. P. Layer-by-Layer Nanoarchitectonics: Invention, Innovation, and Evolution. *Chem. Lett.* **2014**, *43*, 36−68.

(24) Dierendonck, M.; De Koker, S.; De Ryckebc, R.; De Geest, B. G. Just Spray It - LbL Assembly Enters a New Age. *Soft Matter* **2014**, *10*, 804−807.

(25) Qi, W.; Yan, X. H.; Fei, J. B.; Wang, A. H.; Cui, Y.; Li, J. B. Triggered Release of Insulin from Glucose-Sensitive Enzyme Multi-layer Shells. *Biomaterials* **2009**, *30*, 2799−2806.

(26) Cui, W.; Cui, Y.; Zhao, J.; Li, J. B. Fabrication of Tumor Necrosis Factor-Related Apoptosis Inducing Ligand (TRAIL)/ALG Modified $CaCO_3$ as Drug Carriers with the Function of Tumor Selective Recognition. *J. Mater. Chem. B* **2013**, *1*, 1326−1332.

(27) Qi, W.; Wang, A. H.; Yang, Y.; Du, M.; Bouchu, M. N.; Boullanger, P.; Li, J. B. The Lectin Binding and Targetable Cellular Uptake of Lipid-Coated Polysaccharide Microcapsules. *J. Mater. Chem.* **2010**, *20*, 2121−2127.

(28) Donath, E.; Sukhorukov, G. B.; Caruso, F.; Davis, S. A.; Möhwald, H. Novel Hollow Polymer Shells by Colloid-Templated Assembly of Polyelectrolytes. *Angew. Chem., Int. Ed.* **1998**, *37*, 2201−2205.

(29) Caruso, F.; Caruso, R. A.; Möhwald, H. Nanoengineering of Inorganic and Hybrid Hollow Spheres by Colloidal Templating. *Science* **1998**, *282*, 1111−1114.

(30) De Koker, S.; Hoogenboom, R.; De Geest, B. G. Polymeric Multilayer Capsules in Drug Delivery. *Angew. Chem., Int. Ed.* **2010**, *49*, 6954−6973.

(31) Tong, W.; Song, X. X.; Gao, C. C. Layer-by-Layer Assembly of Microcapsules and their Biomedical Applications. *Chem. Soc. Rev.* **2012**, *41*, 6103−6124.

(32) Qi, W.; Duan, L.; Li, J. B. Fabrication of Glucose-Sensitive Protein Microcapsules and their Applications. *Soft Matter* **2011**, *7*, 1571−1576.

(33) Sinani, V. A.; Koktysh, D. S.; Yun, B.; Matts, R. L.; Pappas, T. C.; Motamedi, M.; Thomas, S. N.; Kotov, N. A. Collagen Coating Promotes Biocompatibility of Semiconductor Nanoparticles in Stratified LBL Films. *Nano Lett.* **2003**, *3*, 1177−1182.

(34) Delcea, M.; Möhwald, H.; Skirtach, A. G. Stimuli-Responsive LbL Capsules and Nanoshells for Drug Delivery. *Adv. Drug Delivery Rev.* **2011**, *63*, 730−747.

(35) Choi, J.; Rubner, M. F. Influence of the Degree of Ionization on Weak Polyelectrolyte Multilayer Assembly. *Macromolecules* **2005**, *38*, 116−124.

(36) Skirtach, A. G.; Javier, A. M.; Kreft, O.; Köhler, K.; Alberola, A. P.; Möhwald, H.; Parak, W. J.; Sukhorukov, G. B. Laser-Induced Release of Encapsulated Materials Inside Living Cells. *Angew. Chem., Int. Ed.* **2006**, *45*, 4612−4617.

(37) Lvov, Y.; Antipov, A. A.; Mamedov, A.; Möhwald, H.; Sukhorukov, G. B. Urease Encapsulation in Nanoorganized Micro-shells. *Nano Lett.* **2001**, *1*, 125−128.